

22p
N64-22072

SPHEROIDAL FREE PERIODS OF THE EARTH OBSERVED AT EIGHT
STATIONS AROUND THE WORLD

22072
BY L. E. ALSOP

ABSTRACT

Spectral peaks corresponding to the spheroidal free periods of oscillation of the earth exist in the spectra of eight seismograms written at stations in different parts of the world shortly after the great Chilean earthquake of 22 May 1960. These data have been combined with those previously reported by various authors to obtain a very precise phase velocity vs period curve for Rayleigh waves in the period range of 200 to 3200 seconds. The observed spectral amplitudes lend some support to the assumption of a moving source, but they also indicate that the present theory is not adequate. The vertical motion is found to be symmetric with respect to reflections through the pole.

code none - cat. 12

AUTHOR

INTRODUCTION

The seismograms written by vertical component seismographs at eight stations around the world shortly after the great Chilean earthquake of May 22, 1960, have been Fourier analyzed. The resultant spectra show peaks corresponding to the free oscillations of the earth of the spheroidal type. The stations are all part of the world-wide network of long-period seismographs initially placed in operation during the International Geophysical Year and operated by the Lamont Geological Observatory in cooperation with local institutions. The stations were located at the time of the Chilean shock at Agra, India; Hallett, Antarctica; Hong Kong; Lwiro, Republic of the Congo; Mt. Tsukuba, Japan; Resolute, Cornwallis Island, Northwest Territories, Canada; Suva, Fiji; and Uppsala, Sweden. The vertical component seismographs all consist of 15-second pendulums and 75-second galvanometers.

The spectra of these seismograms are presented in this article together with a tabulation of the periods of the free oscillations observed at each station. For the convenience of the reader all other known data for spheroidal oscillations are also tabulated and an average value calculated for each free period. On the basis of these data it is possible to compute a phase velocity vs period curve for the fundamental Rayleigh mode in the period range of 200 to 3200 seconds. Over much of the period range the phase velocities thus obtained have a standard error of the mean of less than 0.1%. The observed spectral amplitudes are also discussed.

DISCUSSION OF SPECTRA

Table 1 lists the sources of the data used to obtain the spectra together with the epicentral distance from the stations to the epicenter at 39.5°S, 74.5°W, and also the azimuths of the great circle paths between the epicenter and the stations both at the epicenter and at the station. The azimuths are given in degrees clockwise from 0° at true north. As the origin time of the earthquake was 19:11:17, 22 May 1960, table 1 shows that the intervals used for the analysis began between approximately four hours to fifteen hours after the earthquake occurred. In most cases the galvanometers were driven off scale and were reset the following day when the records were changed. This is the primary reason for the different beginning times of the intervals. As much as possible of one complete day's record was used for the analysis.

The seismograms were digitized at Lamont using an instrument designed by Pomeroy described previously by Alsop, Sutton, and Ewing (1961). All of the records were digitized with an interval of approximately six seconds between data points. The exact value of the digitization interval was calculated to three decimal places by dividing the time length of the record by the number of data points. In this way allowance could be made for the stretching or shrinking of the record paper during processing.

Prior to digitizing, the traces were smoothed by eye to remove short period waves, i.e., of the order of 10 to 15 seconds. After digitization, in order to reduce the amount of data to be analyzed, while avoiding aliasing, the data were smoothed by averaging over 19 and 21 points, and then every third point was selected. The data were then

Table 1
Summary of Data

Station	Latitude	Longitude	Epicentral Distance	Azimuth from Epicenter	Azimuth at Station	Record
Agra	27°08'N	78°01'E	154.04°	110.03°	234.64°	07:31:24, 23 May - 02:03:38, 24 May 1960
Hallett	72°18'S	170°18'E	59.84°	198.66°	125.93°	01:42:34, 23 May - 22:22:45, 23 May 1960
Hong Kong	22°18'N	114°10'E	161.32°	205.85°	158.63°	02:19:00, 23 May - 01:26:00, 24 May 1960
Lwiro	2°15'S	28°48'E	98.80°	100.24°	229.63°	10:40:00, 23 May - 05:10:24, 24 May 1960
Mt. Tsukuba	36°12'N	140°06'E	152.58°	274.12°	107.42°	04:44:30, 23 May - 04:05:38, 24 May 1960
Resolute	74°41'N	94°54'W	114.70°	354.14°	162.73°	01:44:41, 23 May - 01:54:49, 24 May 1960
Suva	18°01'S	178°26'E	91.13°	245.38°	132.28°	23:35:40, 22 May - 14:33:16, 23 May 1960
Uppsala	59°51'N	17°38'E	124.15°	37.54°	249.12°	07:46:49, 23 May - 03:01:40, 24 May 1960

Fourier analyzed and the periods of the spectral peaks obtained by interpolation. This is the same procedure described in slightly more detail by Alsop, Sutton, and Ewing (1961).

The spectra for the eight stations are shown in figures 1 through 8 in increasing order of starting time of the seismograms after the earthquake. The periods of the observed free vibrations for the fundamental mode are given in the first eight columns of table 2. The general appearance of each of the spectra is approximately the same. The rapid fall-off of the seismometer sensitivity at long periods limits the longest observed free oscillations to those with periods of about 600 to 700 seconds, i.e., approximately orders 8 or 9 of the spheroidal mode. The shortest period of oscillation observed is approximately 200 seconds. As might be expected, since short period oscillations decay more rapidly with time than the long period oscillations, the spectra of the seismograms starting many hours after the earthquake do not have peaks with as short a period as the spectra of seismograms starting a few hours after the earthquake. The general trend of the decay of the short period energy may be observed by comparing the spectra in figures 1 through 8 with the starting times given in table 1. The highest spectral peaks occur between 300 and 400 seconds for the seismograms with an early beginning while for the seismograms

CASE FILE COPY

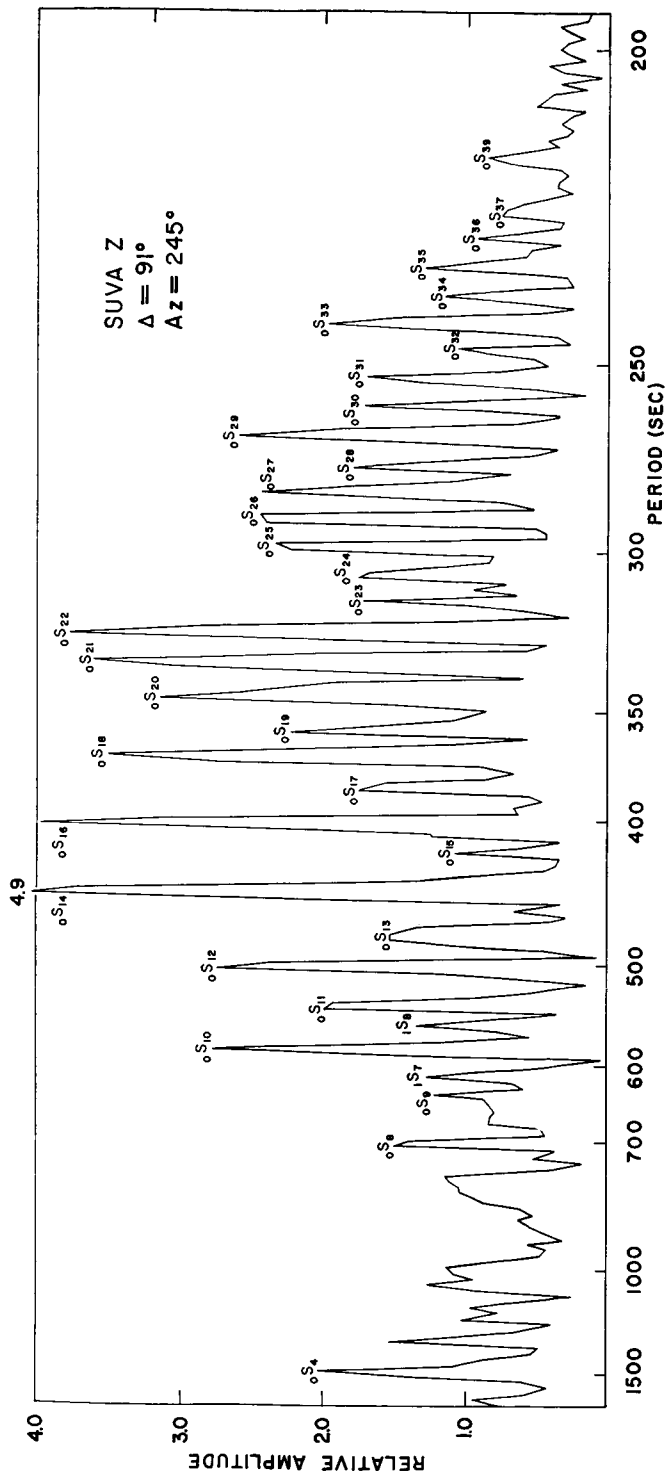


FIG. 1. Spectrum of Suva, Fiji, seismogram.

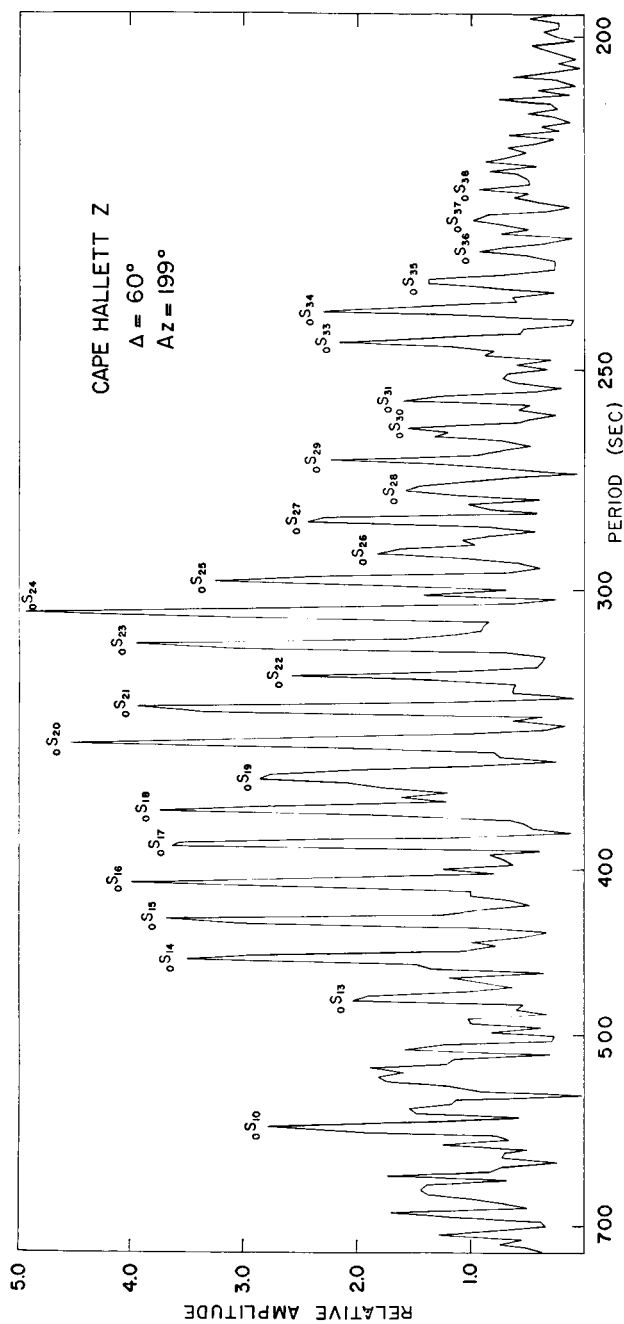


Fig. 2. Spectrum of Hallett, Antarctica, seismogram.

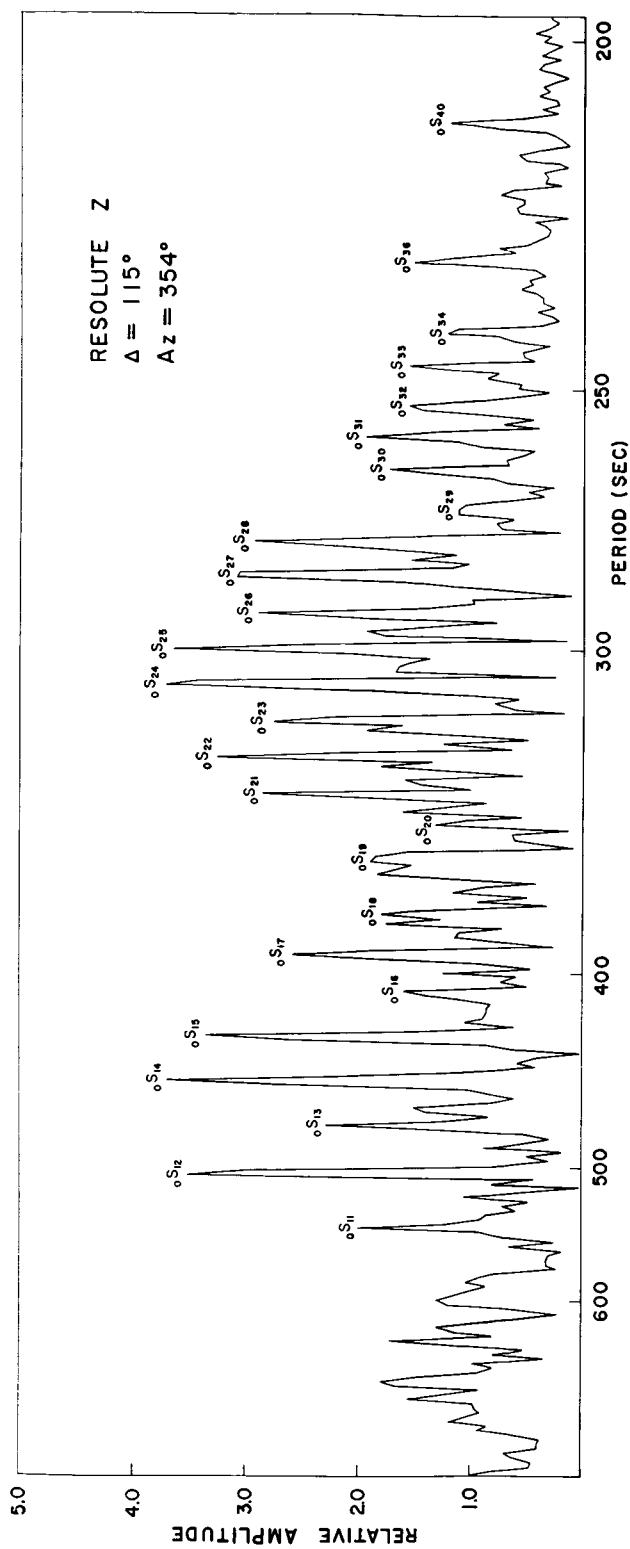


FIG. 3. Spectrum of Resolute, Northern Canadian Islands, seismogram.

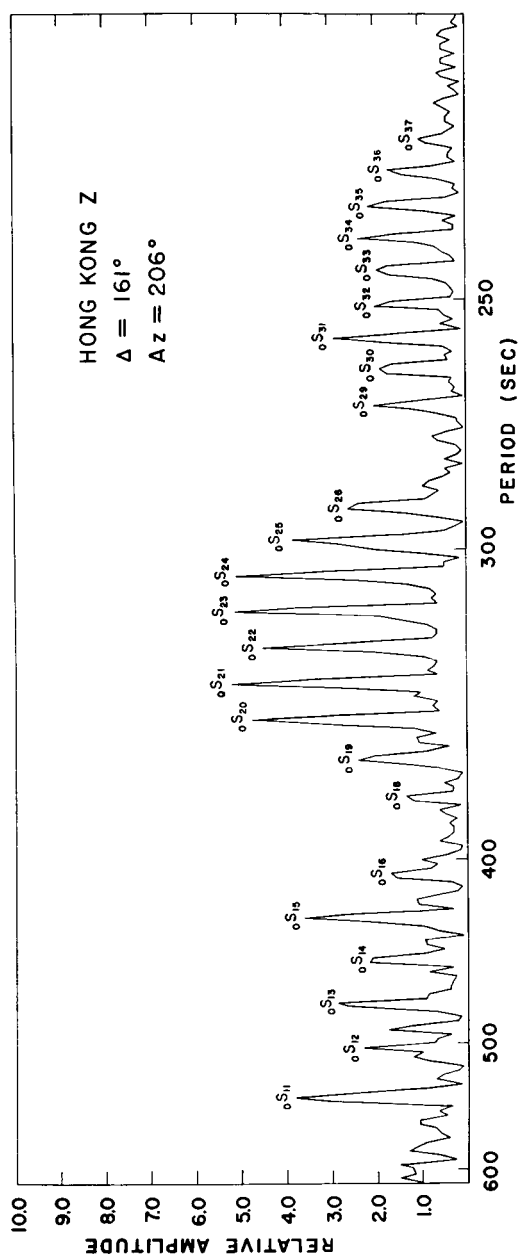


FIG. 4. Spectrum of Hong Kong seismogram.

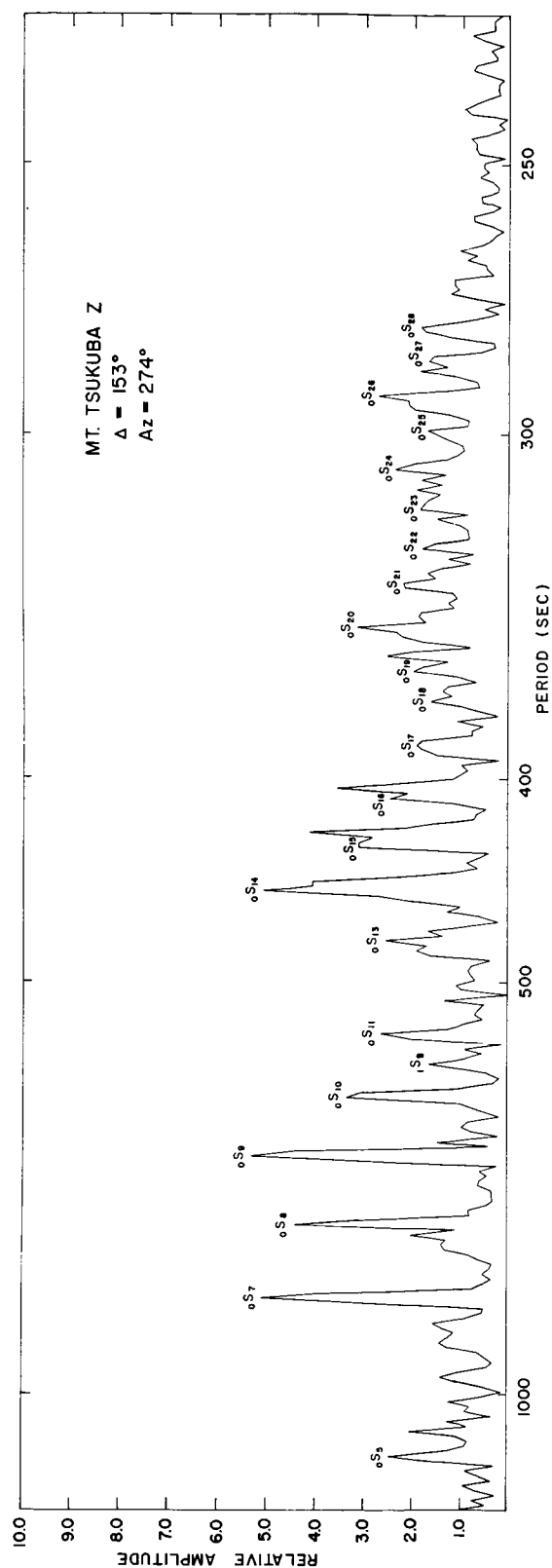


Fig. 5. Spectrum of Mt. Tsukuba, Japan, seismogram.

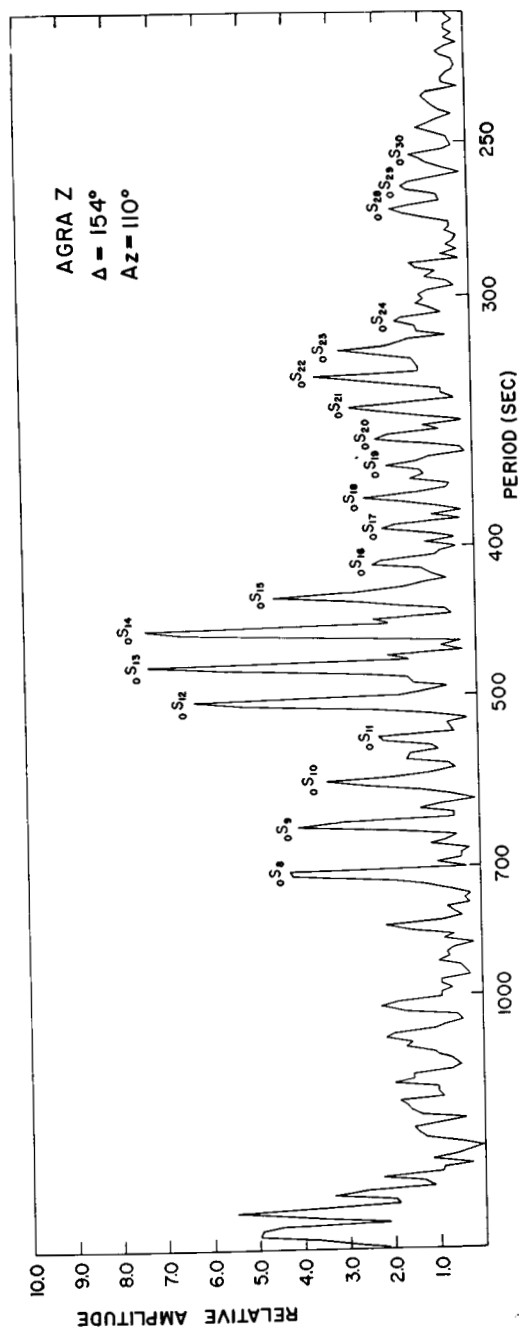


Fig. 6. Spectrum of Agra, India, seismogram.

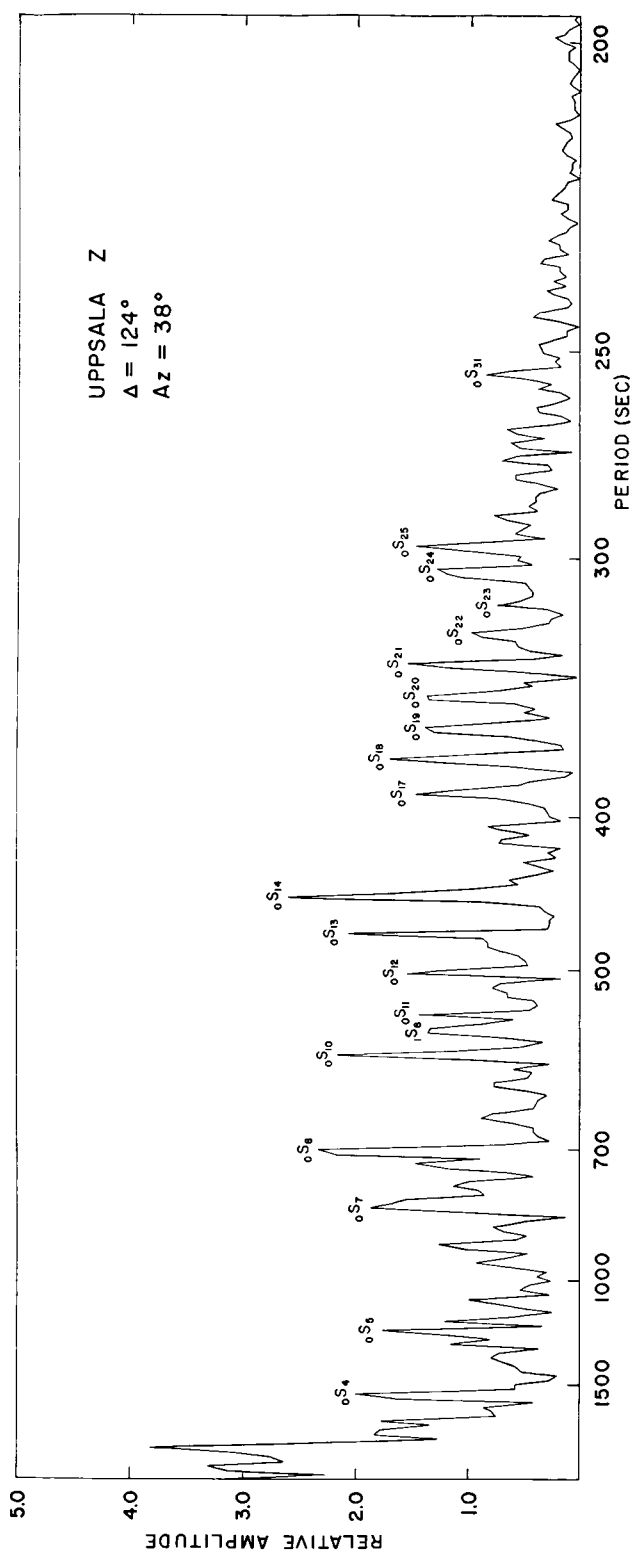


FIG. 7. Spectrum of Uppsala, Sweden, seismogram.

with a later beginning the highest peaks occur between 400 and 500 seconds or even more. The variation of amplitudes between successive peaks will be discussed in more detail in another section of this article.

Spectral peaks corresponding to some of the first higher mode oscillations are observed in the spectra for Suva, Mt. Tsukuba, Lwiro, and Uppsala. The oscillation ${}_1S_8$ is observed in all four spectra and there is a suggestion of a peak corresponding to this oscillation in the Agra spectrum. (N.B. throughout this article the notation of MacDonald and Ness (1961) will be used to identify the various types of free vibrations.) The observed first higher mode oscillations are tabulated in table 3. The highest order observed is possibly 9. This is in accord with theoretical calcula-

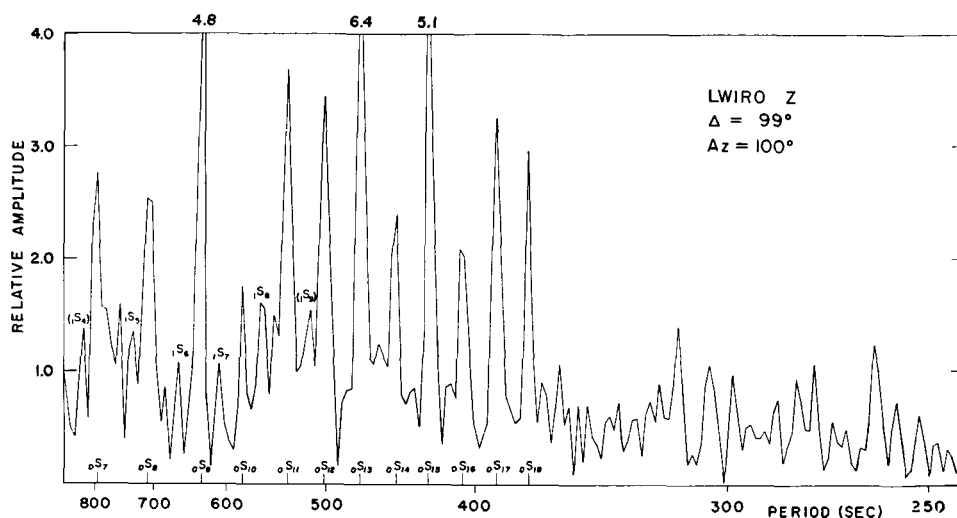


FIG. 8. Spectrum of Lwiro, Republic of the Congo, seismogram.

tions of Alsop (1963) which indicate that the amplitudes of orders 10 through 15 will be small at the surface of the earth. Theoretical periods for the Gutenberg-Bullen B and Gutenberg-Bullen A models from the same article are also included in table 3 for comparison.

OBSERVED PERIODS

Table 2 is a composite of all spheroidal free oscillation data published to date for the fundamental mode. For orders 10 and below of the fundamental mode there can be no confusion in distinguishing spheroidal from torsional oscillations with the exception of ${}_0S_7$ and ${}_0T_7$ so that all of the data available were used for these orders. For orders higher than 10 it becomes difficult to positively identify a spectral peak as belonging to a spheroidal or to a torsional oscillation on the basis of period alone. Accordingly, for orders higher than 10, only data obtained by vertical seismographs or by gravimeters, both of which can only record spheroidal oscillations, were used.

The data selected in accordance with the above criterion, in addition to those reported in this article, were taken from the following: Ness, Harrison, and Slichter

Table 2
Summary of Observed Free Periods of Spheroidal Oscillations, Fundamental Mode

Mt. Tsukuba	Lwipo	Suva	Uppsala	Hong Kong	Jalilott	Agra	Resolute*	Chester	Tiefenort	Trieste	Paris	Kyoto	Palisades	Los Angeles Pasadena	Average
oS2								326.4		318.6		320.4	325.2	323.3	322.9 ± 12
oS3								212.4		217.2		214.8	214.9	213.4	214.3 ± 7
oS4		(1486)	(1577)					153.0	154.8	155.4	155.2	153.0	155.0	155.1	154.5 ± 3
oS5	(1177)		1191					117.6	118.2	118.8	119.4	119.4	119.7	119.0	118.9 ± 2
oS6	(945)							95.6		96.0	96.5	96.2	96.6	96.4	96.2 ± 1
oS7	809		809					80.6			(816)	81.2	(816)	80.5	80.9 ± 1
oS8	706	708	706			710		70.7	70.8	70.8	70.7	70.7	70.4	70.7	70.7 ± 1
oS9	631	636				637		63.2			63.5	63.4	63.4	63.4	63.4 ± 1
oS10	578	580	579		579	583		57.6				58.1	57.2	58.1	57.9 ± 1
oS11	532	536	538	539		538	541	53.6				53.6	53.3	53.6	53.6 ± 1
oS12		502.6	502.3	501.5	502.5	504.5	502.9	501.0				503.1	501.4	502.1	502.3 ± 0.3
oS13	474.5	473.6	(478.5)	473.0	474.5	475.6	473.7	472.2					471.7	472.9	473.4 ± 0.3
oS14	448.4	449.0	447.6	446.8	449.4	450.0	449.4	448.2					447.6	448.1	448.3 ± 0.3
oS15	427.0	426.7	(423.0)		427.2	428.5	427.5	424.2					426.6	426.1	426.5 ± 0.4
oS16	406.7	408.2	406.7	(407.0)	406.9	409.2	407.7	405.0					406.7	406.8	407.0 ± 0.4
oS17	(386.4)	390.0	388.3	388.7	388.8	390.1	392.1	390.0					390.0	389.3	389.3 ± 0.3
oS18	(370.9)	374.7	373.5	372.6	(375.7)	375.4	(376.6)	375.0					374.1	373.9	374.1 ± 0.3
oS19	360.9	360.5	362.2	359.4	361.6	361.0	(362.1)	360.0						360.1	360.7 ± 0.3
oS20	(348.0)		348.3	346.9	348.3	349.2	346.3	346.2					346.9	346.7	347.4 ± 0.3
oS21	335.8		336.0	334.8	336.8	335.6	337.2	336.0					335.2	336.5	335.9 ± 0.2
oS22	325.6		325.0	(323.9)	326.0	324.8	326.9	325.2					325.1	325.4	325.2 ± 0.3
oS23	(315.7)	315.7	314.9	(314.2)	316.2	315.4	317.3	315.0					315.2	315.3	315.5 ± 0.2
oS24	306.7	305.6	305.9	305.2	306.9	306.1	(307.2)	306.0					306.6	306.2	306.1 ± 0.2
oS25	(298.5)	298.5	297.2	296.9	298.4	297.4	299.8	297.6					297.4	297.5	297.6 ± 0.2
oS26	(291.0)		289.1		290.5	290.1	292.0	290.4					289.4	289.7	289.9 ± 0.3
oS27	(283.6)	280.7	281.8		282.2	282.2	283.7	282.6					281.4	282.2	281.8 ± 0.3
oS28	(277.7)	276.3	274.7		275.0	(275.8)	277.0	275.4					274.4	275.1	275.2 ± 0.3

* - Resolute data not included in averages (see text).

Table 2 (Continued)

Mt. Tasukuba	Summary of Observed Free Periods of Spheroidal Oscillations										Fundamental Mode				
	Swva	Uppsala	Hong Kong	Hallett	Agra	Resolute ^a	Chester	Tiefenort	Trieste	Patia	Kyoto	Palisades	Los Angeles	Pasadena	Average
σ_{S29}	267.9		269.1	268.4	(270.1)	(271.3)	268.2				267.7	268.6	268.2	268.3 \pm 0.3	
σ_{S30}	261.8		262.6	(261.9)	(262.8)	263.7	261.6					255.4	256.2	256.0 \pm 0.2	
σ_{S31}	257.1		256.7	256.0		257.9	255.0				249.2	250.0	250.8	250.1 \pm 0.3	
σ_{S32}	249.7		251.0			253.0						245.3	244.8	245.1 \pm 0.2	
σ_{S33}	244.5		245.5	245.2		246.4	245.4				238.7	239.9	240.0	239.6 \pm 0.2	
σ_{S34}	239.2		240.2	239.6		241.2	239.4					235.2	235.2	234.9 \pm 0.3	
σ_{S35}	233.9		235.3	234.7											
σ_{S36}	228.8		230.4	(229.9)		231.1					230.7	230.2	229.2	229.9 \pm 0.4	
σ_{S37}	224.7		(226.0)	(225.0)			225.0				226.9	225.3	223.8	225.1 \pm 0.5	
σ_{S38}				(220.4)							219.2	220.9	219.6	219.9	
σ_{S39}	216.1										214.9	216.7		215.9	
σ_{S40}						213.5					211.5			211.5	
σ_{S41}											207.3	208.5		207.3	
σ_{S42}											204.3	204.3		204.3	

^a - Resolute data not included in averages (see text).

(1961), designated as Los Angeles in the table; Benioff, Press, and Smith (1961), designated as Pasadena; Bogert (1961) designated as Chester; Alsop, Sutton, and Ewing (1961) designated as Palisades although only the data for orders greater than seven were obtained on a vertical seismograph at Palisades, the remainder being recorded on the first Lamont strain seismograph at Ogdensburg, New Jersey; Buchheim and Smith (1961) designated as Tiefenort; Bolt (1963) designated as Trieste; Connes, Blum, Jobert, and Jobert (1962) designated as Paris; and Takeuchi, Saito, Kobayashi, and Nakagawa (1962) designated as Kyoto. All of the periods are given in seconds for the purposes of table 2, although originally much of the data were given in minutes.

The average value of these data are also given in table 2. The data contained in parentheses were not used in obtaining the average because of the unsatisfactory appearance of the peaks in the spectra. The standard error of the mean is also given

Table 3
Observed Free Periods of Spheroidal Oscillations, First Higher Mode

	<u>Suva</u>	<u>Mt. Tsukuba</u>	<u>Lwiro</u>	<u>Uppsala</u>	<u>Average</u>	<u>Gutenberg Bullen B</u>	<u>Gutenberg Bullen A</u>
$1S_4$			(840.3)		(840.3)	864	847
$1S_5$			738.9		738.9	740	723
$1S_6$			663.8		663.8	666	649
$1S_7$	611.4		608.8		610.1	611	596
$1S_8$	555.7	553.2	559.9	553.2	555.4	560	547
$1S_9$			(514.6)		(514.6)	511	501

for each average value for orders 2 through 37. Above order 37 the data are too meager to attempt any statistical analysis. Over much of the range of periods given, the standard error of the mean is approximately one part in a thousand.

The values of period obtained from the analysis of the Resolute seismogram are not included in the average. After the averages and standard errors were computed it was found that the Resolute values were consistently high. The value of χ^2 was calculated (Jeffreys, 1948) and was found to be 60.589 for 22 degrees of freedom. Tables of χ^2 (Fisher and Yates, 1943) indicate that the probability of χ^2 being greater than 48.268 is less than .001. On this basis the data were rejected as containing a large systematic error, presently unknown, and the averages and standard errors were recalculated. These are the values which appear in table 2.

PHASE VELOCITIES

From the periods of the free spheroidal oscillations given in table 2, the phase velocities, C , of the fundamental Rayleigh mode may be calculated by use of the following relation:

$$C = \frac{2\pi a}{(n + \frac{1}{2})T} \quad (1)$$

where a is the radius of the earth, n the order number of the free oscillation, and T the period. This is an approximate formula. As discussed in Alsop (1963), for orders less than 10 the value of phase velocity obtained is the instantaneous phase velocity at an epicentral distance of 90° .

The phase velocities calculated from the averages of the observed free oscillations are listed in table 4 together with the error calculated from the standard error of

Table 4
Phase Velocities of Fundamental Rayleigh Mode

	Period (sec)	Phase Velocity (km/sec)		Period (sec)	Phase Velocity (km/sec)
$0S_2$	3229	$4.959 \pm .018$	$0S_{23}$	315.5	$5.399 \pm .003$
$0S_3$	2143	$5.337 \pm .018$	$0S_{24}$	306.1	$5.338 \pm .004$
$0S_4$	1545	$5.754 \pm .011$	$0S_{25}$	297.6	$5.275 \pm .004$
$0S_5$	1189	$6.121 \pm .010$	$0S_{26}$	289.9	$5.211 \pm .005$
$0S_6$	962	$6.402 \pm .006$	$0S_{27}$	281.8	$5.165 \pm .006$
$0S_7$	809	$6.597 \pm .008$	$0S_{28}$	275.2	$5.104 \pm .006$
$0S_8$	707	$6.661 \pm .009$	$0S_{29}$	268.3	$5.058 \pm .006$
$0S_9$	634	$6.646 \pm .011$	$0S_{30}$	261.9	$5.011 \pm .004$
$0S_{10}$	579	$6.584 \pm .011$	$0S_{31}$	256.0	$4.964 \pm .004$
$0S_{11}$	536	$6.494 \pm .012$	$0S_{32}$	250.1	$4.925 \pm .006$
$0S_{12}$	502.3	$6.375 \pm .004$	$0S_{33}$	245.1	$4.875 \pm .004$
$0S_{13}$	473.4	$6.264 \pm .004$	$0S_{34}$	239.6	$4.843 \pm .004$
$0S_{14}$	448.3	$6.158 \pm .004$	$0S_{35}$	234.9	$4.800 \pm .006$
$0S_{15}$	426.5	$6.055 \pm .005$	$0S_{36}$	229.9	$4.770 \pm .008$
$0S_{16}$	407.0	$5.961 \pm .006$	$0S_{37}$	225.1	$4.742 \pm .010$
$0S_{17}$	389.3	$5.876 \pm .005$	$0S_{38}$	219.9	4.728
$0S_{18}$	374.1	$5.784 \pm .005$	$0S_{39}$	215.9	4.694
$0S_{19}$	360.7	$5.691 \pm .005$	$0S_{40}$	211.5	4.673
$0S_{20}$	347.4	$5.621 \pm .005$	$0S_{41}$	207.3	4.653
$0S_{21}$	335.9	$5.543 \pm .003$	$0S_{42}$	204.3	4.610
$0S_{22}$	325.2	$5.471 \pm .005$			

the mean of the free period averages. Figure 9 is a plot of the phase velocities as a function of period. The phase velocities are obtained of course only at the periods of the free oscillations. The curve is achieved by interpolating graphically. At each of the points obtained from the free oscillations the error is also indicated. For purposes of comparison phase velocity curves obtained from the calculated free periods of oscillation for two earth models are also included (Alsop, 1963). The models both have velocities according to Gutenberg but one has the densities of Bullen's Model A while the other has the densities of Bullen's Model B.

It can be seen from figure 9 that for periods greater than 1100 seconds the phase velocities calculated from the observed free periods of oscillation agree very well

with those calculated from the Gutenberg-Bullen B model. For periods less than 1100 seconds the observed phase velocity diverges from that of the Gutenberg-Bullen B model and tends towards the phase velocity curve of the Gutenberg-

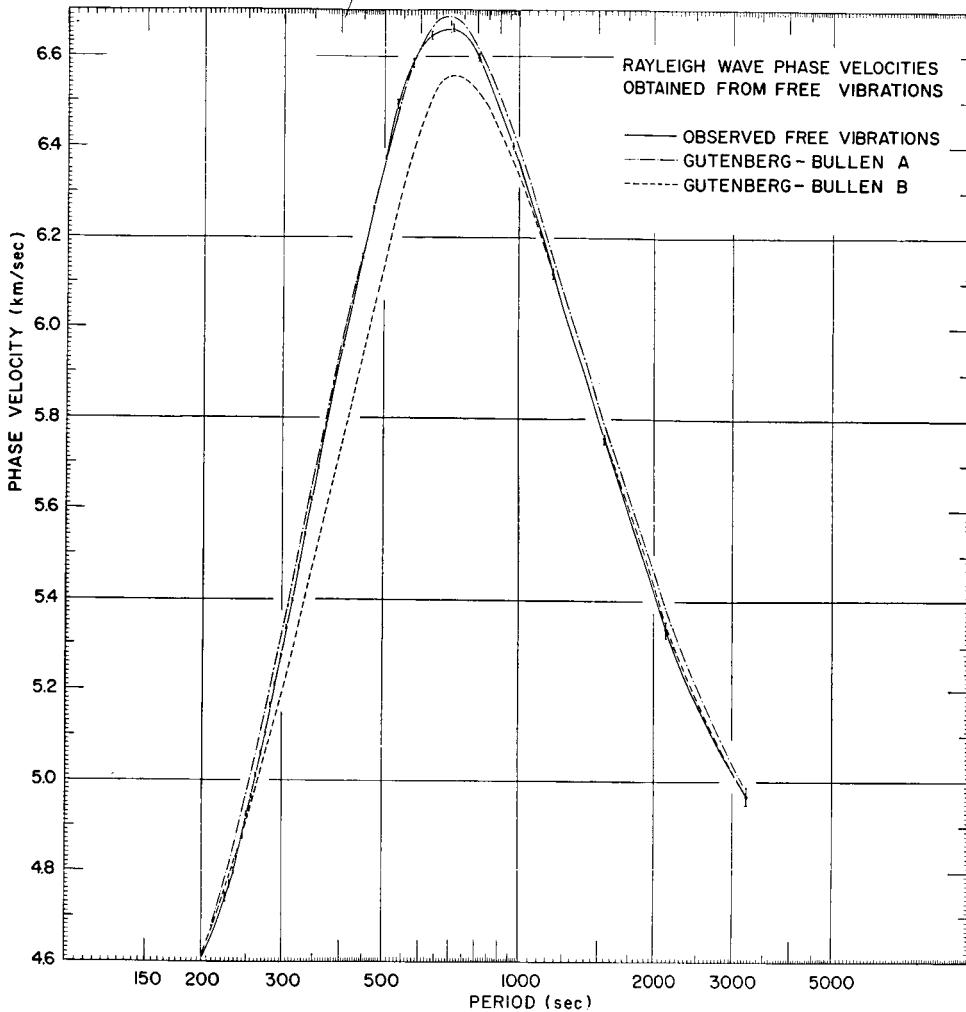


FIG. 9. Comparison of Rayleigh wave phase velocities above 200 seconds obtained from observed free periods of oscillation with two earth models. (Bars on either side of observed phase velocity points indicate limits of the standard error of the mean.)

Bullen A model, finally meeting with the curve of the Bullen A model at about 550 seconds. The observed curve follows the theoretical curve for the Gutenberg-Bullen A model, at first slightly below, then slightly above until about 400 seconds. In this period range the variations from the theoretical curve are only slight but they are consistent and do not show any random character. Below 400 seconds the observed phase velocities diverge downwards from the theoretical phase velocities. Once again they approach the Gutenberg-Bullen B model but cross over this phase

velocity curve and near 230 seconds the observed phase velocities are lower than those calculated for either model. The observed phase velocities of table 4 in the period range of 220 to 340 seconds are in excellent agreement with values obtained from surface waves by Brune, Benioff, and Ewing (1961).

It would appear from the fact that both density models yield phase velocities which are higher than the observed phase velocities in the period range of 200–240 seconds that the fault lies with the velocity model used. This is not too surprising. Approximately three-quarters of the path for a free oscillation is oceanic, while the Gutenberg velocity model is continental. The "path" of a free oscillation is taken to be the path of the two opposing surface waves which form the standing wave pattern.

Using a modification of the program SPHOS 3 described in Alsop (1963), which makes possible the calculation of the free periods of oscillation for earth models with a surficial liquid layer, phase velocities have been calculated for the oceanic model Case 122 of Sykes, Landisman, and Satô (1962). The results which are summarized in table 5 are disappointing. The phase velocities obtained are even higher than those calculated for the two continental models. This model gave excellent results for both oceanic Rayleigh and Love waves in the period range of 30 seconds to 150 seconds.

Finally it is of interest to compare the few observed free periods of the first higher mode with the theoretical values as shown in table 3. All of the observed free periods lie closer to the calculated periods of the Bullen B model than to those of the Bullen A model. This is to be expected. Orders 6 through 9 of the fundamental mode do have phase velocities more like those of the Bullen A model as the period decreases, but the higher mode oscillations have appreciable amplitudes at greater depths than those of the fundamental mode. Therefore the higher mode oscillations can be expected to favor the same model as do the lower orders of the fundamental mode.

SPECTRAL AMPLITUDES

The vertical amplitudes of the free vibrations of a sphere as a function of position on the surface of the sphere vary as $P_n^m(\cos \theta)e^{im\phi}$ (Morse and Feshbach, 1953), where θ is the colatitude and ϕ the azimuth angle. For the free vibrations of the earth excited by an earthquake, the logical place to choose the pole is at the epicenter of the earthquake. For point sources of a simple type—point compressional, couple, etc.—it seems reasonable to expect with this choice for the pole that the motion for each order n will be characterized by the same degree m or at least by a sum of even or of odd m 's of the same symmetry.

The relative amplitudes of the Legendre polynomials P_n were calculated for the different epicentral distances given in table 1 using the formula for the asymptotic behavior of the Legendre function (Jahnke and Emde, 1945):

$$P_n(\cos \theta) = \sqrt{\frac{2}{\pi n \sin \theta}} \left[\left(1 - \frac{1}{4n}\right) \sin \Theta - \frac{1}{8n} \cot \theta \cos \Theta \right] \quad (2)$$

where $\Theta = (n + \frac{1}{2})\theta + \pi/4$. A comparison of the calculated values with the spectral peaks of the same order showed no similarity. In particular, peaks were found

to be missing in the spectra where the Legendre polynomial of that order should have appreciable amplitude and were found to be present where the Legendre polynomial of that order would have an almost null amplitude. Comparing the

Table 5
Free Periods and Phase Velocities
of Spheroidal Oscillations, Fundamental Mode
Case 122

	Period (sec)	Phase Velocity (km/sec)
$0S_{18}$	370.9	5.832
$0S_{19}$	356.8	5.753
$0S_{20}$	343.9	5.678
$0S_{21}$	332.1	5.606
$0S_{22}$	321.2	5.538
$0S_{23}$	311.3	5.472
$0S_{24}$	302.0	5.410
$0S_{25}$	293.4	5.350
$0S_{26}$	285.3	5.293
$0S_{27}$	277.8	5.240
$0S_{28}$	270.7	5.188
$0S_{29}$	264.0	5.139
$0S_{30}$	257.7	5.093
$0S_{31}$	251.7	5.049
$0S_{32}$	246.0	5.007
$0S_{33}$	240.5	4.967
$0S_{34}$	235.4	4.929
$0S_{35}$	230.4	4.892
$0S_{36}$	225.7	4.859
$0S_{37}$	221.2	4.825
$0S_{38}$	216.8	4.795
$0S_{39}$	212.6	4.765
$0S_{40}$	208.6	4.737
$0S_{41}$	204.8	4.710
$0S_{42}$	201.1	4.684

missing peaks of the spectra with the predicted zero points of the Legendre polynomials or the associated Legendre polynomials at the epicentral distance is the simplest test which will definitely show if the spectral peaks do not have amplitudes similar to polynomials of a given degree m . Therefore the zero point curves for P_n^1 and P_n^2 of Satô and Usami (1963), who proposed this method, were used to determine if the spectra might obey these types of distribution. Again no correspondence was observed.

The magnification of the seismograph as a function of period will cause the ratio of the amplitudes to be different from that predicted by considering the relative amplitudes of the Legendre polynomials only, but since the magnification curve is a smooth curve over these period ranges, it will not introduce peaks and valleys into the spectra. Also the time variation of the source must be considered, but for periods as long as the free vibrations the spectral characteristics of the source due to the time variation should be represented by a smooth curve, most likely monotonically decreasing with increasing period.

In order to explain the difference in phase shift between the vertical and horizontal motion for different orders of oscillation, Benioff, Press, and Smith (1961) postulated a moving source, i.e., faulting with a finite rupture velocity. They found that the observed phase shifts were best explained by rupture velocities of 3 to 4 km/sec and fault lengths of 960 to 1280 km. These authors derived the following expression for the amplitude μ_n of the vertical motion of the n th order oscillation with angular frequency σ_n due to a moving source:

$$\mu_n \approx \int_0^\infty P_n[\cos(\theta - \epsilon \cos A)] \sin \left[\sigma_n \left(t - \frac{a\epsilon}{C_0} \right) \right] d\epsilon \quad (3)$$

where θ_0 is the angular fault length, ϵ is the angular variable along the fault, θ is the angular epicentral distance, C_0 is the rupture velocity, a is the earth's radius, and A is the angle between the great circle through the fault and the great circle from the station to the epicenter.

Using expression (3), the relative amplitudes to be expected at the epicentral distances given in table 1 were calculated for fault lengths of 960 and 1200 km and a rupture velocity of 4 km/sec. Comparison with the spectra showed some similarity at the long periods, i.e., greater than 400 seconds, but not at the short periods.

The discussion up to now has concerned all of the spectra shown in figures 1 through 8, considered as a group. However, the spectra of Suva, figure 1, is of interest by itself. The distance from the epicenter to Suva is slightly more than 90° . From (2) it can be seen that near 90° the Legendre polynomials of odd order are small for small n . At the epicentral distance of Suva, they become as large as the even order polynomials for n equal to about 37. Formula (2) may be generalized for the associated Legendre polynomials (Hobson, 1931) to

$$P_n^m(\cos \theta) = (-n)^m \left(1 - \frac{m(m+1)}{2n} \right) \sqrt{\frac{2}{n\pi \sin \theta}} \left[\left(1 + \frac{m^2}{2n} - \frac{1}{4n} \right) \cdot \sin \left(\Theta + \frac{m\pi}{2} \right) - \frac{1}{2n} \left(m^2 - \frac{1}{4} \right) \cot \theta \cos \left(\Theta + \frac{m\pi}{2} \right) \right] \quad (4)$$

where again $\Theta = (n + \frac{1}{2})\theta + \pi/4$. Formula (4) shows that the odd order polynomials will also be small near 90° for associated Legendre polynomials of even degree m , while the even orders will be small for the polynomials of odd degree. Figure 1 shows that the odd peaks of the spectra for Suva are indeed smaller than the even peaks up to order 21. This tends to indicate that the source has primarily

Table 6
Comparison of Observed Spectral Amplitudes of Suva Spectrum
with Calculated Amplitudes for Moving Source

	<u>Observed</u>	<u>Fault Length = 960 km</u>	<u>Fault Length = 1200 km</u>
$0S_8$	1.6	6.4	8.8
$0S_9$	1.2	1.1	2.3
$0S_{10}$	2.8	5.9	7.4
$0S_{11}$	2.2	1.3	2.7
$0S_{12}$	2.9	5.1	6.0
$0S_{13}$	1.6	1.5	3.1
$0S_{14}$	4.9	4.5	4.9
$0S_{15}$	1.2	1.8	3.3
$0S_{16}$	4.0	4.0	4.0
$0S_{17}$	1.8	2.0	3.5
$0S_{18}$	3.6	3.5	3.2
$0S_{19}$	2.3	2.1	3.5
$0S_{20}$	3.7	3.0	2.7
$0S_{21}$	3.8	2.3	3.5
$0S_{22}$	3.8	2.6	2.3
$0S_{23}$	1.9	2.4	3.4
$0S_{24}$	1.9	2.2	2.1
$0S_{25}$	2.6	2.5	3.2
$0S_{26}$	2.7	1.9	1.9
$0S_{27}$	2.1	2.5	3.0
$0S_{28}$	1.8	1.7	1.8
$0S_{29}$	2.7	2.5	2.7
$0S_{30}$	1.8	1.5	1.7
$0S_{31}$	1.8	2.5	2.3
$0S_{32}$	1.1	1.4	1.6
$0S_{33}$	1.9	2.4	2.0
$0S_{34}$	1.1	1.3	1.4
$0S_{35}$	1.2	2.3	1.6
$0S_{36}$	1.0	1.2	1.2
$0S_{37}$	0.8	2.2	1.2
$0S_{38}$	-	1.1	0.9
$0S_{39}$	0.9	2.0	0.8

an even symmetry with respect to ϕ , the azimuthal angle, since the surface solutions are of the form $P_n^m(\cos \theta)e^{im\phi}$, where m must be the same in both terms because it is a separation constant arising in the separation of the scalar wave equation in spherical coordinates. The calculations for the moving source show that the effect

is to reduce the order at which the amplitudes of the even and odd order polynomials become equal. For a source length of 960 km and a rupture velocity of 4 km/sec the even and odd orders should have equal orders at Suva at approximately order 23 and for a fault length of 1200 km with the same rupture velocity at approximately order 17. Therefore, to this extent, the spectra of Suva, where the even and odd order amplitudes become equal at about order 21, could be explained by motion along a fault of the dimensions and with a velocity of that suggested by Benioff, Press, and Smith. However, further details of the spectrum beyond order 21 are not in good agreement with the amplitudes predicted for the moving source. For purposes of comparison the relative amplitudes predicted for the two different fault lengths, for $m = 0$, are given in table 6 together with the observed amplitudes. The calculated amplitudes have been multiplied by a proportionality constant, so that the amplitudes for ${}_0S_{16}$ are equal. Also the asymptotic value formula for the P_n 's given in (2) has been multiplied by $\sqrt{n + \frac{1}{2}}$ to give a normalization in which $\int [P_n(x)]^2 dx = 1$, where $x = \cos \theta$, (Sommerfeld, 1958). Table 6 shows that for a fault length somewhere between 960 and 1200 km the agreement with the observed amplitudes is quite good up to order 21, which has a period of 336 seconds, allowing for the fact that the sensitivity of the seismograph is low at the long period end of the spectrum and consequently the signal-to-noise ratio of the spectrum is small for the long periods. There is a trough at $n = 23$ and 24 which does not occur for the calculated amplitudes. Both calculated amplitudes for $n = 26$ are small; the observed amplitude is large. Other discrepancies may be noted for higher orders.

One possible reason for the lack of agreement between the observed and calculated amplitudes at the shorter periods for this spectrum and also for the other seismograms may be contamination of the spectrum at the shorter periods by some of the aftershocks. Another possibility is that while the concept of the moving source may be correct, the assumption implicit in (3) that the intensity of the radiated energy is uniform all along the fault is open to question. A varying intensity of radiation along the fault should have the greatest effect on the short period end of the spectrum where the wave lengths are short.

CONCLUSIONS

Spectral peaks corresponding to the free periods of oscillation of the earth have been found in the spectra of eight seismograms obtained from vertical seismographs located at various stations around the world. From these and previously reported values of the free periods of spheroidal type oscillations, it has been possible to obtain very precise values of Rayleigh wave phase velocities in the period range of 200 to 3200 seconds. While the phase velocity curve agrees with that predicted for several earth models over different parts of its period range, it does not agree with any existing model over its entire extent. This phase velocity curve should be a valuable aid to the problem of modifying existing earth models. Similar data for the torsional oscillations would also be valuable and it is hoped that it will be possible to obtain these from the horizontal seismograms of these stations. The difficulty lies in positively identifying a peak in the spectrum of a horizontal seismogram as being definitely a torsional or a spheroidal free period.

The observed amplitudes of the spectra do not agree well with those predicted

for simple point sources. The assumption of a moving source tends to explain the observed amplitudes at periods greater than 400 seconds, but not for shorter periods than this. It is suggested that variations in the intensity of the radiation emitted by the source as a function of time might explain the discrepancies at short periods.

The peaks of the spectrum of Suva, which are alternately large and small, as is to be expected for a station slightly greater than 90° distant from the epicenter, indicate that the vertical motion is primarily symmetric with respect to reflections through the epicenter. Presumably, the source mechanism must be of this same symmetry.

ACKNOWLEDGMENTS

The author wishes to thank the personnel at the eight seismographic stations who obtained the data used for this research. Professor Y. Satô of the Earthquake Research Institute of the University of Tokyo kindly made available his figures of the zero points of the associated Legendre polynomials prior to publication. The author acknowledges helpful discussions with Professors Jack Oliver and George H. Sutton and Drs. James N. Brune and Mark Landisman of the Lamont Geological Observatory.

This research was supported in part through the Air Force Cambridge Research Laboratories under Contract AF 19(604) 7376 as part of the Advanced Research Projects Agency's Project VELA-UNIFORM.

REFERENCES

- Alsop, L. E., G. H. Sutton, and M. Ewing
1961. "Free Oscillations of the Earth Observed on Strain and Pendulum Seismographs," *J. Geophys. Res.*, 66: 631-641.
- Alsop, L. E.
1963. "Free Spheroidal Vibrations of the Earth at Very Long Periods, Part I—Calculation of Periods for Several Earth Models," *Bull. Seis. Soc. Am.*, 53: 483-501.
- Benioff, H., F. Press, and S. Smith
1961. "Excitation of the Free Oscillations of the Earth by Earthquakes," *J. Geophys. Res.*, 66: 605-619.
- Bogert, B. P.
1961. "An Observation of Free Oscillations of the Earth," *J. Geophys. Res.*, 66: 643-646.
- Bolt, B. A.
1963. "Revised Torsional Eigenperiods from the 1960 Trieste Data," *Geophysical Journal*, 7: 510-512.
- Brune, J. N., H. Benioff, and M. Ewing
1961. "Long-Period Surface Waves from the Chilean Earthquake of May 22, 1960, Recorded on Linear Strain Seismographs," *J. Geophys. Res.*, 66: 2895-2910.
- Buchheim, W. and S. W. Smith
1961. "The Earth's Free Oscillations Observed on Earth Tide Instruments at Tiefenort, East Germany," *J. Geophys. Res.*, 66: 3608-3610.
- Connes, J., P. A. Blum, G. et N. Jobert
1962. "Observation des Oscillations proposees de la Terre," *Ann. de Geophysique*, 18: 260-268.
- Fisher, R. A. and F. Yates
1943. *Statistical Tables for Biological, Agricultural, and Medical Research*, Table IV, Oliver & Boyd, Edinburgh.
- Hobson, E. W.
1931. *The Theory of Spherical and Ellipsoidal Harmonics*, Cambridge Univ. Press, p. 304.
- Jahnke, E. and F. Emde
1945. *Tables of Functions*, 4th ed., Dover, New York, p. 117.
- Jeffreys, H.
1948. *Theory of Probability*, 2nd ed., Oxford, p. 87-92.
- MacDonald, G. J. F. and N. F. Ness
1961. "A Study of the Free Oscillations of the Earth," *J. Geophys. Res.*, 66: 621-629.

Morse, P. M. and H. Feshbach

1953. *Methods of Theoretical Physics, Part II*, McGraw-Hill Book Company, New York, p. 1872-4 and 1898-1900.

Satô, Y. and T. Usami

1963. "Method of Determining the Degree of Free Oscillation of a Radially Heterogeneous Elastic Sphere," *Bull. Earthquake Res. Inst.*, 41: 341-342.

Sommerfeld, A.

1958. *Partielle Differential gleichungen der Physik*, 4th ed., Akademische Verlagsgesellschaft, Leipzig, p. 20-24.

Sykes, L., M. Landisman, and Y. Satô

1962. "Mantle Shear Wave Velocities Determined from Oceanic Love and Rayleigh Wave Dispersion," *J. Geophys. Res.*, 67: 5257-5271.

Takeuchi, H., M. Saito, N. Kobayashi, and I. Nakagawa

1962. "Free Oscillations of the Earth Observed on Gravimeters," *Geophysical Notes*, 15: Contribution No. 22 (also *Zisin. Sec. II*, 15: 122-137, 1962).

LAMONT GEOLOGICAL OBSERVATORY

COLUMBIA UNIVERSITY

PALISADES, NEW YORK

Contribution No. 692

AND

GODDARD INSTITUTE FOR SPACE STUDIES

NATIONAL AERONAUTICS AND SPACE ADMINISTRATION

NEW YORK, NEW YORK

Manuscript received November 18, 1963.